JETIR.ORG ISSN: 2349-5162 | ESTD Year : 2014 | Monthly Issue
JOURNAL OF EMERGING TECHNOLOGIES AND INNOVATIVE RESEARCH (JETIR)
An International Scholarly Open Access, Peer-reviewed, Refereed Journal

PIXE: Instrumentation

G. J. Naga Raju
Associate Professor
Department of Physics,
Department of Physics, JNTU-GVCEV, Vizianagaram 535003, India.

Abstract: Particle Induced X-ray Emission (PIXE) is a well-recognized nondestructive method for analyzing samples for their elemental content. Due to its high sensitivity, multi-elemental analysis capability, non-destructive nature, ability to analyze tiny samples and suitability for a wide range of samples, this technique has served as an important tool for elemental analysis. The X-ray emission spectrum obtained in PIXE serves as a blue print for identifying and quantifying elements. The energies of the characteristic peaks help in identifying the elements and their intensities help in quantifying those elements. Several elements in the periodic table, starting from Na can be determined simultaneously in the ppm range using this versatile technique. The present work is aimed to elaborate the various steps involved in the PIXE analytical technique in detail.

Index Terms **– PIXE, X-rays, Analytical technique.**

I. INTRODUCTION

Johansson et al. (1970) first demonstrated PIXE at the Lund Institute of Technology in 1970. It is a reliable technique that is utilized for elemental analysis. It is highly sensitive technique with a capability to analyze simultaneously several elements from Na to U in very small quantities of sample within a short time. Additionally, large X-ray production Cross-section, low bremsstrahlung and matrix effects and high signal to noise ratio make this technique suitable for detection of trace elements at 1 ppm or less. The main advantage of the technique is that sample can be reused for the further studies i.e, it is non-destructive technique.

PIXE technique is applied for elemental analysis in all possible fields (scientific or technical) from the past four decades. Trace elemental analysis has been successfully carried out the in the coal samples of Singareni and Talcher coal samples using PIXE by Srikanth et al (S. Srikanth and G. J. Naga Raju, 2019). PIXE is employed for the quantitative study of trace elements in coal and coal related ashes collected from NTPC, Visakhapatnam (S. Srikanth and G. J. Naga Raju, 2019). Concentrations of elements K, Ca, Ti, V, Cr, Mn, Fe, Co, Cu, Zn, Se, Br, Rb, and Sr were determined in the serum samples of healthy and breast caner patients using the PIXE (B. Gowri Naidu et al, 2020).The regional variation of elemental content has studied by analyzing the Cyperus rotundus plant collected from different geographical locations by PIXE and ICP-MS(J. Chandra Sekhar Rao et al, 2019). Chemometric analysis has been carried out on the trace elemental data in the samples of biological and medicinal plants using PIXE analytical technique (Rao et al, 2019 and Naidu et al., 2019).

Biological reference materials of NIST SRM Bovine Liver (1577c) and IAEA RM Animal Blood (A-13) were analysed using PIXE and compared with standard values. The experimental results were consistent with the NIST and IAEA certified values (B. Gowri Naidu et al, 2018). Ravi Kumar et al (M. Ravi Kumar, 2015) analysed soils samples collected from the geographically at different locations using the PIXE. The observed high level of concentrations of some elements compared to the control area is attributed to automotive exhaust and industries in the vicinity. To know the alterations of the elements in the blood sera of cervical cancer patients with respect to the health controls, serum samples of controls as well as cancer patients were analysed by employing PIXE technique (Sarita et al 2014). Hair and Nail samples of psychiatric and cervical cancer patents were also analyzed using PIXE analytical technique.

PIXE technique comprises of two parts. One is to identify the elements present in the sample target from X-rays energies of the characteristic peaks in the X-ray emission spectrum and the other is to quantify the elements present in the target from the intensity of its characteristic X-ray emission spectrum. This normally requires knowledge of the ionization cross-sections, fluorescence yields, radiative transition widths and absorption coefficients.

2. BASIC PRINCIPLE OF PIXE

When the ion beam with sufficient energy interacts with the target atoms, X-rays are emitted via de-excitation process. While the collision takes place the incident ions may experience elastic or inelastic scattering. Under ion bombardment the target atom of a sample loses inner-shell electrons. Outer-shell electrons then fill the inner-shell vacancies and the transitions are followed by emission of X-rays corresponding to energy difference between the two shells. The X-rays thus emitted characterize the excited atom. This is illustrated schematically in Figure 1. The transition of an outer shell electron to a particular shell of the target atom such as the K, L or M shell results in emission of that particular X-ray i.e., the K, L or M line respectively. The area under the peaks is proportional to the concentrations.

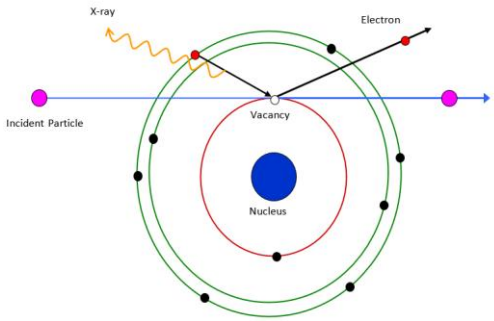

Fig. 1 Schematic representation of Principle Underlying PIXE

3. INSTRUMENTATION OF PIXE

The instrumentation of PIXE involves the use of a beam of protons which can be acquired from low energy tandem Pelletron accelerator. The quadrupole magnets were used to monitor the beam dynamics. A beam of 3 MeV protons, collimated to 2 mm diameter by using a graphite collimator were made to strike the target placed on a sample ladder in the scattering chamber. The pressure within the scattering chamber was maintained at 10^{-6} mbar. The proton beam was incident on targets placed at 45^0 angle to the beam. When these protons interacted with target atoms, the X-rays of elements in the target were emitted. These characteristic X-rays were registered with a Si(Li) detector having energy resolution of 160 eV FWHM at 5.9 keV. The detected X-ray signals were processed by a multichannel analyzer and transferred to a personal computer. Faraday cup was used to measure the charge collected on the target sample. Figure 2 shows the block diagram of instrumentation for PIXE technique.

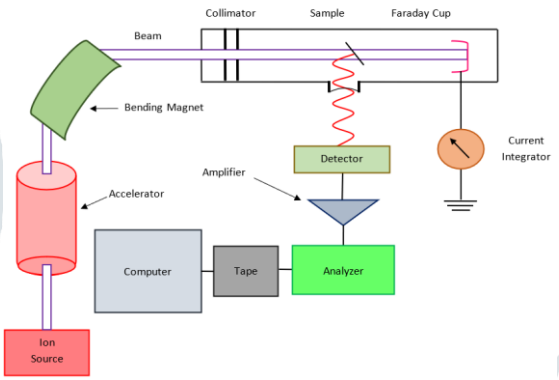

Fig. 2 Instrumentation of PIXE

3.1 TANDEM PELLETRON ACCELERATOR

A 3 MV tandem Pelletron accelerator, two ion sources i.e., an Alphatross source and a SNICS sputter source, and six beam lines make up the accelerator facility at IBL. Solid or liquid cesium was heated in the SNICS to form vapour. The positively charged cesium ions which were formed from the cesium vapour stream were accelerated to reach the end of the cathode. The cathode was made of pressed TiH_2 powder which was used to generate protons. The atoms of hydrogen that were sputtered got ionized and then accelerated through an aperture present in the ionizer. To focus the extracted beam an Einzel lens was used. The source bias was a pre-acceleration section through which the focused beam passes. An injector magnet was used to select the desired species. The beam gets the necessary energy from the bias voltage which allows for a good species resolution by the injector magnet. The injector magnet then directs the beam to another

Einzel lens. A set of x-y magnetic steerers further inject the beam into the high voltage tank. At the center of the accelerated tube there is a positively charged terminal towards which the beam of negative ions gets accelerated on entering the accelerator tube. An even voltage gradient was maintained along the tube up to the terminal within the accelerator column enclosing the tube with the terminal at a maximum voltage of 3MV. Two nylon chains with steel pellets in each link were used to deliver the charge to the terminal. A small quantity of nitrogen gas was launched into the vacuum in the terminal space to remove the electrons from the beam at the center of the terminal. Neutral, single and multiple charged positive ions were produced as a result of collisions between nitrogen gas molecules and ion beam. The ground potential which was located at the end of the accelerator further accelerates the quick moving positively charged beam particles till they exit from the accelerator. The high voltage terminal was electrically insulated by filling the tank space enclosing the accelerated tube with SF_6 gas and constantly keeping it at 65-70 psi pressure. Turbo pumps, titanium ion pumps and cryo-pumps kept at periodic intervals along the length of the beam line were used to maintain the vacuum inside the accelerating tube.

A switching magnet was used to guide the ions of a particular charge into separate beam lines. Magnetic elements like dipoles and quadrupoles were used for the energy analysis, focusing and deflection of the beam. The pre-acceleration stage (bias voltages, extractor and cathode), the charge of the ion (selected by the switching magnet) and the terminal voltage of the accelerator results in the energy of the beam at the target. In the target chamber, a quadrupole magnetic lens and additional steering was used to guide the focused ion beam onto the target. In this study the protons had incident ion energy of 3 MeV when they reached the

beam line located at 0° to the accelerator. The beam of 2 mm diameter at a current of 10 - 40 nA was allowed to focus on the target. All the functions like beam production, transportation to the target were controlled by the computer operations as it was easy and fast to reproduce the experimental set up and tuning processes.

3.2 SCATTERING CHAMBER

Scattering Chamber is the most important part in accelerator based experiments. The scattering chamber is octagonal in shape with 20" diameter and 15" height and consists of several ports for X-ray and γ-ray detectors. A Si(Li) detector connected to one of the ports of the scattering chamber close to the target so as to ensure a wide solid angle, was used to identify the X-rays. There is a viewing window in the scattering chamber which allows to view the location and the size of the beam spot and thus helps in focusing the beam sharply onto the target. The target was positioned at 45° angle with respect to both the detector and the incident beam direction. The scattering chamber was usually maintained at low vacuum (~ 10^{-6} Torr) during the measurements by using rotary and diffusion pumps. The beam current was measured and focused right onto the target as the targets were electrically conductive. To monitor the beam current, the target holder was directly coupled to the charge integrator in the current study.

3.3 TARGET MOUNTING ARRANGEMENT

The samples were loaded on an octagonal shaped aluminium target ladder, with a facility to load 48 samples at a time. This avoids the necessity to repeatedly open and re-evacuate the scattering chamber. The target holder, on which the samples were loaded, was placed on a sample manipulator that was fastened to the scattering chamber's top port. The samples were then irradiated in vacuum. Position of beam on sample could be changed externally without breaking the vacuum by rotating the sample manipulator in the desired direction.

3.4 DATA ACQUISITION AND ELECTRONICS SYSTEMS

The characteristic X-rays released from different samples as a consequence of the ion-atom collision processes were identified by Si(Li) detector. The X-rays passed through a 30 mm air gap, a 12.7 μm beryllium detector window and a 95 μm metallized Mylar chamber window before entering the active volume of the detector. There was a distance of 62 mm between the Si(Li) detector's active volume and the target. Ortec power supply (Model 459) was used for applying a negative bias of 450V to the detector. Block diagram of the electronics systems employed in the present experiment is shown in Figure 3.

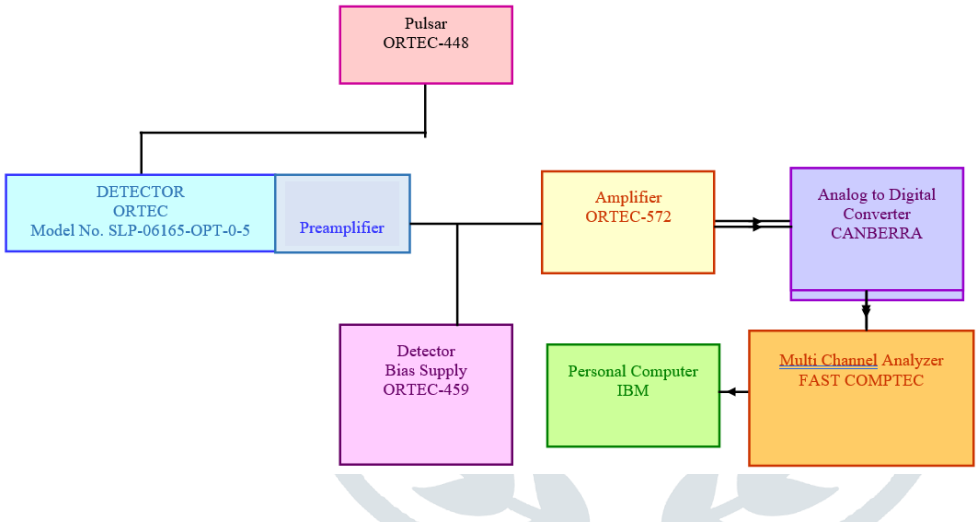

Fig. 3 Block Diagram of electronics used in the data acquisition system used for PIXE

The electronic modules were assembled as per the block diagram. The characteristic X-rays were detected after they passed through the scattering chamber's Mylar Window. An aluminium aperture of fixed size was placed facing the Si(Li) detector for exactly measuring the solid angle subtended by the detector at the beam position on the sample's surface. The signals from the detector preamplifier were processed using an ORTEC-572 spectroscopic amplifier, to enable pile-up rejections, and subsequently sent into a Canberra ADC. Storage and data manipulation were performed using a Canberra S100 counting system which works on an IBM personal computer. Spectral data was sent to a computer where additional data analyses were performed. ORTEC-448 research pulsar was attached to the counting system for observing the spectrum's stability.

3.5 Si(Li) DETECTOR

Si(Li) detectors have wide spread use in the applied as well as fundamental research areas of physics. For detecting X-rays emitted from a radioactive source, an X-ray tube or an accelerator, the Si(Li) detector serves as a highly sensitive research tool with superior performance. A cooled field effect transistor (FET), cooled lithium drifted silicon crystal, high gain and low noise preamplifier, liquid nitrogen (LN_2) dewar, cryostat with a Be window, and cable pack form the detector system. The Si(Li) detector consists of a 12.7 μm thick Be window with an active area of 12.5 mm^2. There is a provision for automatic shut off to prevent the FET from getting damaged when LN_2 supply drops during high voltage operation.

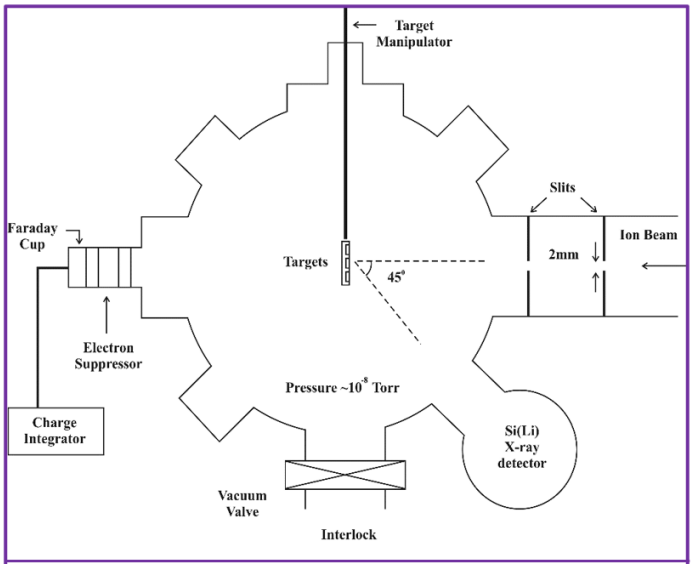

Fig. 4 Schematic Diagram of the Scattering Chamber

3.6 Role of Si(Li) Detector in PIXE Experiments

As the HPGe or Ge(Li) detectors posses maximum efficiency up to 100 keV, they can be used to detect the K X-rays of high 'Z' elements accurately. On the other hand, as 'Z' increases the K X-ray cross section for protons decreases. Hence K X-rays of high 'Z' elements are seldomly detected in PIXE while using Ge detectors. Rather than using the K X-rays to detect high Z elements, L X-rays are widely used as their energy appropriately matches with the range of maximum efficiency 2 to 20 keV of Si(Li) detector. Hence, from the resulting spectrum in PIXE for a muti-element sample, the low Z ($Z < 50$) and high Z ($Z \geq 50$) elements are identified by their K X-ray and L X-ray energies respectively. Moreover, a single setting of the detector makes it capable of recording simultaneously the spectrum of all the elements in the sample.

3.7 Energy Calibration

PIXE spectrum is highly complicated as it has a composite mix of L X-ray lines and K X-ray lines. Detection of every element in the PIXE spectrum depends on the detector's accuracy in energy calibration. Radioactive sources ^{241}Am and ^{55}Fe provided by International Atomic Energy Agency (IAEA) were used for calibrating the Si(Li) detector. It was observed that the L X-ray and K X-ray components of the afore-mentioned isotopes were well resolved and the centroid of each photo peak was determined as shown below

$$X_c = \sum (X_i \, . Y_i) / \sum Y_i$$
$$Y_c = \sum (X_i \, . Y_i) / \sum X_i$$

where X_i and Y_i are the channel number and the count rate, X_c and Y_c are the centroid coordinates. The net count rate was calculated after subtracting the background. In general GUPIXWIN software package was used for subtracting the background and determining the peak centroid. Using the relation $y = mx + c$ the resultant points of the standard lines were fitted. The constants m and c were determined using the least squares method and by using the values of m and c, the energies of the unknown X- ray lines were calculated.

3.8 Detector System - Resolution Characteristics

Detector's resolution capability is of prime importance for the X-ray spectra analysis especially in case of L X-ray spectra. The term used to express the resolution of solid state detector is full width at half maximum (FWHM) of a standard line. In this study the Si(Li) detector's resolution was determined at 5.9 keV K X-ray energy of ^{55}Mn. A standard Fe-55 source was placed at 5 cm distance from the window of the detector so as to accomplish a dead time of the order of 1%. The spectrum of K X-rays from Fe-55 source was registered by the detector for a prolonged period so as to ensure good statistical results. The FWHM of the resulting spectrum was ascertained at an optimum time constant of the amplifier. 160 eV at 5.9 keV energy was the resolution of the Si(Li) detector used in the current study.

3.9 Si(Li) Detector - Efficiency

Both fundamental and applied research requires a Si(Li) detector which is accurately calibrated for its efficiency. A Si(Li) detector with very good resolution was used for detecting the low energy X-rays (1-20 keV) which were emitted from the elements present in the samples under study as a result of proton bombardment. The fundamental parameter of the detector is its counting efficiency. The intrinsic efficiency of a detector is stated as the number of pulses recorded out of the number of radiation quanta incident on the detector. The solid angle Ω subtended by the detector at the beam spot on the sample's surface can be obtained with good accuracy since there is an Al aperture in front of the detector. The detector can see a fraction $\Omega/4\pi$, of the total number of photons released during the process. Therefore, this fraction $\Omega/4\pi$ called geometrical factor is also considered in addition to the intrinsic efficiency of the detector. Hence, the detector's intrinsic efficiency can be calculated as $\varepsilon_d = \varepsilon/\varepsilon_{geo}$, where ε is the total efficiency of detection and ε_{geo} is the geometrical efficiency that is dependent on the geometric parameters related to the experimental setup of the detector.

The detector parameters as given by the manufacturer were used to calculate theoretically the intrinsic efficiency of Si(Li) detector. Intrinsic efficiency ε_d is calculated as follows

$$\varepsilon_d(E) = e^{-(\mu_{Be}.X_{Be} + \mu_{Au}.X_{Au} + \mu_{Si}.\Delta x_{Si})} \cdot (1 - e^{-\mu_{Si}.X_{Si}})$$

where μ's are the coefficients of absorption of Be window, gold (Au) layer on Si crystal and Si(Li) crystal itself respectively at the X-ray energy E, X's are the thickness of the Be window. Au layer and Si(Li) crystal, and Δx_{Si} represents the thickness of the Si(Li) crystal's insensitive part. The values for thicknesses, i.e., X values, were provided by the manufacturer and XCOM computer code (*Berger and Hubbell, 1987*) was used to find out the absorption coefficients. The total efficiency of the detector, made up of the detector's intrinsic efficiency, it's solid angle and X-ray attenuation factor for absorption between its intrinsic region and target, was measured by the procedure as detailed by *Pajek et al. (1989)*.

Data on K-shell ionization cross-sections by protons showing good agreement (within experimental uncertainties) with the K-shell ionization data of the ECPSSR theory is found abundantly in literature (*Orlic et al., 1994).* The efficiency of the Si(Li) detector used in this work was estimated by replacing the K X-ray production cross-sections with the K-shell ionization cross-sections for the elements Ca, V, Fe, Cu and Zn, by using 3 MeV protons. From the ISICS code the theoretical ionization cross sections were taken (*Liu and Cipolla, 1996).*

The experimental detector efficiency is calculated using the formula

$$\varepsilon_d = \frac{4\Pi Y_x \sigma_R(\theta) \Delta\Omega_p}{\varepsilon_t \varepsilon_a Y_R \Delta\Omega_x \sigma_K^x} \left(\frac{t_x}{t_R}\right)$$

where,

σ_k^x = K X-ray theoretical production ionizations from ISICS code, Y_x (θ) = Measured K X-ray yieldY_R (θ) = Measured Rutherford yield, σ_R (θ) = Differential Rutherford scattering cross-section,ε_d = Si(Li) detector intrinsic efficiency, ε_a = Absorption correction for Mylar chamber window and air path, ε_t = Correction due to self absorption of the target thickness $\Delta\Omega_p$ = Solid angle subtended by the charged particle silicon surface barrier detector,$\Delta\Omega_x$ = Solid angle subtended by the Si(Li) X-ray detector. t_x = Dead time correction for X-ray counting, t_R = Dead time correction for charged particle counting

Fig. 5 shows the theoretical curve which represents the estimated efficiency points obtained in the current study. It was inferred that within the experimental uncertainties the estimated efficiency points were in accordance with the theoretical values. This shows the dependability of the used efficiency curve.

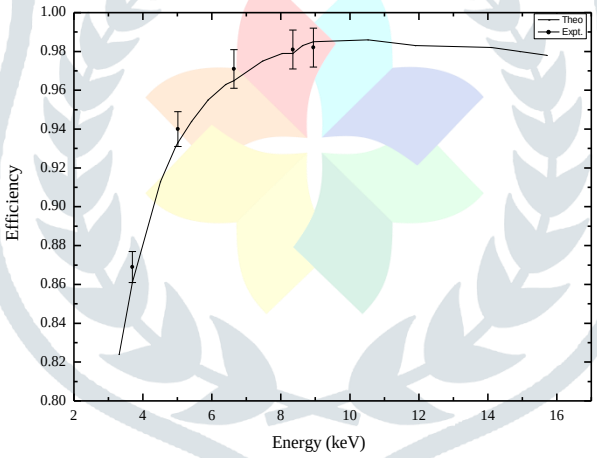

Fig. 5 Variation of Efficiency with Energy

4. Conclusion

Particle Induced X-ray Emission (PIXE) is a accelerator based analytical technique. PIXE is a relatively simple and powerful analytical technique. It can be used to determine the several elements simultaneously even if the specimen is in minute in quantities and because of its nondestructive nature, this technique can be used in several areas of research. Low energy accelerators are used to accelerate protons in general to irradiate the sample and solid-state detectors record the x-rays emitted from the sample. Data acquisition system converts the pulse amplitude signal into digital number with help of Multi-Channel Analyzer to process the X-ray spectrum further.

5. Acknowledgment

The author thankful to the authorities of Institute of Physics, Bhubaneswar, India for providing Ion Beam facilities to carryout the PIXE experiment for the last two decades. The author also thanks the scientific officers and technical team for their constant support during the experimentation.

REFERENCES

[1]. Johansson, T.B., Akselsson, R., Johansson, S. A. E. 1970. Particle Induced X-Ray Emission. Nucl. Instr. and Meth. 84:141-143.
[2]. Srikanth, S., and G. J. Naga Raju. 2020. A comparison study of Singareni and Talcher coal samples through elemental analysis using PIXE technique. Journal of Radioanalytical and Nuclear Chemistry 323(3): 1317-1328.
[3]. Srikanth, S., and GJ Naga Raju. 2019. Quantitative Study of Trace Elements in Coal and Coal Related Ashes using PIXE. Geological Society of India. 94(5): 533-537.
[4]. Naidu, B. Gowri, et al. 2020. PIXE analysis of blood serum of breast cancer patients undergoing successive chemotherapy. Journal of Radioanalytical and Nuclear Chemistry. 323(3): 1307-1316.
[5]. Rao, J. Chandrasekhar, et al. 2019. Quantitative elemental analysis of Cyperus rotundus medicinal plant by PIXE and ICP-MS techniques. " Indian Journal of Pure and Applied Physics 57(9): 671-674
[6]. Rao, J. C., et al. 2019. Elemental analysis of Pterocarpus santalinus by PIXE and ICP-MS: chemometric approach." Journal of Radioanalytical and Nuclear Chemistry. 322: 129-137.
[7]. Naidu, B. Gowri, et al. 2019. Multivariate analysis of trace elemental data obtained from blood serum of breast cancer patients using SRXRF. Results in Physics 12: 673-680.
[8]. B. Gowri Naidu, G. J. Naga Raju P. Sarita.2018. PIXE Analysis of NIST and IAEA Biological Reference Materials. International Journal of Multidisciplinary 3: 221-226,
[9]. Kumar, M. R., et al. 2015. Trace elemental analysis of soil samples using Particle Induced X-ray Emission technique. Journal of Environmental Research and Development 10(2): 298-303.
[10]. Sarita, P., G. J. Naga Raju, and S. Bhuloka Reddy. 2014. Studies on changes in trace elemental content of serum of uterine cervix cancer patients using PIXE. Journal of Radioanalytical and Nuclear Chemistry 302: 1501-1506.
[11]. Pradeep, A. S., et al. 2014. Trace elemental distribution in the scalp hair of bipolars using PIXE technique. *Medical hypotheses* 82(4): 470-477.
[12]. Charles, M. John, et al. 2004. Effect of radiation therapy on trace elemental concentrations of hair samples of cervical cancer patients—PIXE technique. X-Ray Spectrometry 33(6): 410-413.
[13]. Berger, Martin J., and John Howard Hubbell. 1987.XCOM: Photon cross sections on a personal computer. No. NBSIR-87-3597. National Bureau of Standards, Washington, DC (USA). Center for Radiation Research,.
[14]. Pajek, M., Kobzev, A. P., Sandrick, R., Ilkhamov, R. A., Khusmurodov, S.H. 1989.Accurate efficiency determination of a Si(Li) detector in the Si-k and Au-M absorption edge energy region. Nucl. Instr. Meth. Phys. Res. B. 22: 346-358.
[15]. Orlic, I., Snow, C.H., Tang, S.M., 1994. Experimental L-shell X-ray production and ionization cross sections for proton impact. At. Data and Nucl. Data Tables, 56: 159-210.
[16]. Liu, Z., Cipolla, S., 1996. ISICS. A program for calculating K-, L- and M-shell cross sections from ECPSSR theory using a personal computer. Comput. Phy. Comm. 97: 315-330.